This paper is published as part of a *PCCP* themed issue series on biophysics and biophysical chemistry:
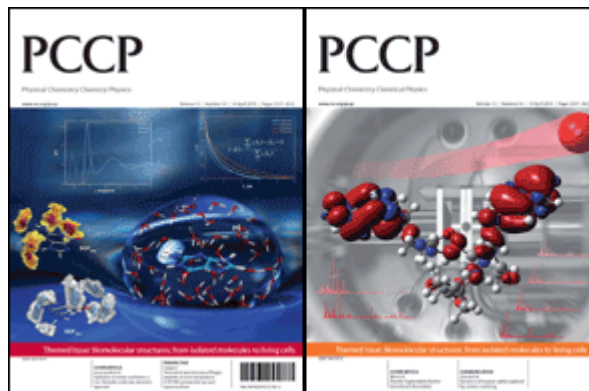
Biomolecular Structures: From Isolated Molecules to Living Cells

**Guest Editors: Seong Keun Kim,
                        Jean-Pierre Schermann and
                        Taekjip Ha**

Editorial

Biomolecular Structures: From Isolated Molecules to the Cell Crowded Medium
Seong Keun Kim, Jean-Pierre Schermann, Taekjip Ha, *Phys. Chem. Chem. Phys.*, 2010

Perspectives

Theoretical spectroscopy of floppy peptides at room temperature. A DFTMD perspective: gas and aqueous phase
Marie-Pierre Gaigeot, *Phys. Chem. Chem. Phys.*, 2010

Communications

Dynamics of heparan sulfate explored by neutron scattering
Marion Jasnin, Lambert van Eijck, Michael Marek Koza, Judith Peters, Cédric Laguri, Hugues Lortat-Jacob and Giuseppe Zaccai, *Phys. Chem. Chem. Phys.*, 2010

Papers

Infrared multiple photon dissociation spectroscopy of cationized methionine: effects of alkali-metal cation size on gas-phase conformation
Damon R. Carl, Theresa E. Cooper, Jos Oomens, Jeff D. Steill and P. B. Armentrout, *Phys. Chem. Chem. Phys.*, 2010

Structure of the gas-phase glycine tripeptide
Dimitrios Toroz and Tanja van Mourik, *Phys. Chem. Chem. Phys.*, 2010

Photodetachment of tryptophan anion: an optical probe of remote electron
Isabelle Compagnon, Abdul-Rahman Allouche, Franck Bertorelle, Rodolphe Antoine and Philippe Dugourd, *Phys. Chem. Chem. Phys.*, 2010

A natural missing link between activated and downhill protein folding scenarios
Feng Liu, Caroline Maynard, Gregory Scott, Artem Melnykov, Kathleen B. Hall and Martin Gruebele, *Phys. Chem. Chem. Phys.*, 2010

Vibrational signatures of metal-chelated monosaccharide epimers: gas-phase infrared spectroscopy of Rb^{+}-tagged glucuronic and iduronic acid
Emilio B. Cagmat, Jan Szczepanski, Wright L. Pearson, David H. Powell, John R. Eyler and Nick C. Polfer, *Phys. Chem. Chem. Phys.*, 2010

Stepwise hydration and evaporation of adenosine monophosphate nucleotide anions: a multiscale theoretical study
F. Calvo and J. Douady, *Phys. Chem. Chem. Phys.*, 2010

Reference MP2/CBS and CCSD(T) quantum-chemical calculations on stacked adenine dimers. Comparison with DFT-D, MP2.5, SCS(MI)-MP2, M06-2X, CBS(SCS-D) and force field descriptions
Claudio A. Morgado, Petr Jurečka, Daniel Svozil, Pavel Hobza and Jiří Šponer, *Phys. Chem. Chem. Phys.*, 2010

Photoelectron spectroscopy of homogeneous nucleic acid base dimer anions
Yeon Jae Ko, Haopeng Wang, Rui Cao, Dunja Radisic, Soren N. Eustis, Sarah T. Stokes, Svetlana Lyapustina, Shan Xi Tian and Kit H. Bowen, *Phys. Chem. Chem. Phys.*, 2010

Sugar–salt and sugar–salt–water complexes: structure and dynamics of glucose–KNO_3–$(H_2O)_n$
Madeleine Pincu, Brina Brauer, Robert Benny Gerber and Victoria Buch, *Phys. Chem. Chem. Phys.*, 2010

Hydration of nucleic acid bases: a Car–Parrinello molecular dynamics approach
Al'ona Furmanchuk, Olexandr Isayev, Oleg V. Shishkin, Leonid Gorb and Jerzy Leszczynski, *Phys. Chem. Chem. Phys.*, 2010

Conformations and vibrational spectra of a model tripeptide: change of secondary structure upon micro-solvation
Hui Zhu, Martine Blom, Isabel Compagnon, Anouk M. Rijs, Santanu Roy, Gert von Helden and Burkhard Schmidt, *Phys. Chem. Chem. Phys.*, 2010

Peptide fragmentation by keV ion-induced dissociation
Sadia Bari, Ronnie Hoekstra and Thomas Schlathölter, *Phys. Chem. Chem. Phys.*, 2010

Structural, energetic and dynamical properties of sodiated oligoglycines: relevance of a polarizable force field
David Semrouni, Gilles Ohanessian and Carine Clavaguéra, *Phys. Chem. Chem. Phys.*, 2010

Studying the stoichiometries of membrane proteins by mass spectrometry: microbial rhodopsins and a potassium ion channel
Jan Hoffmann, Lubica Aslimovska, Christian Bamann, Clemens Glaubitz, Ernst Bamberg and Bernd Brutschy, *Phys. Chem. Chem. Phys.*, 2010
DOI: 10.1039/b924630d

Sub-microsecond photodissociation pathways of gas phase adenosine 5´-monophosphate nucleotide ions
G. Aravind, R. Antoine, B. Klærke, J. Lemoine, A. Racaud, D. B. Rahbek, J. Rajput, P. Dugourd and L. H. Andersen, *Phys. Chem. Chem. Phys.*, 2010
DOI: 10.1039/b921038e

DFT-MD and vibrational anharmonicities of a phosphorylated amino acid. Success and failure
Alvaro Cimas and Marie-Pierre Gaigeot, *Phys. Chem. Chem. Phys.*, 2010
DOI: 10.1039/b924025j

Infrared vibrational spectra as a structural probe of gaseous ions formed by caffeine and theophylline
Richard A. Marta, Ronghu Wu, Kris R. Eldridge, Jonathan K. Martens and Terry B. McMahon, *Phys. Chem. Chem. Phys.*, 2010
DOI: 10.1039/b921102k

Laser spectroscopic study on (dibenzo-24-crown-8-ether)– water and –methanol complexes in supersonic jets
Satoshi Kokubu, Ryoji Kusaka, Yoshiya Inokuchi, Takeharu Haino and Takayuki Ebata, *Phys. Chem. Chem. Phys.*, 2010
DOI: 10.1039/b924822f

Macromolecular crowding induces polypeptide compaction and decreases folding cooperativity
Douglas Tsao and Nikolay V. Dokholyan, *Phys. Chem. Chem. Phys.*, 2010
DOI: 10.1039/b924236h

Electronic coupling between cytosine bases in DNA single strands and i-motifs revealed from synchrotron radiation circular dichroism experiments
Anne I. S. Holm, Lisbeth M. Nielsen, Bern Kohler, Søren Vrønning Hoffmann and Steen Brøndsted Nielsen, *Phys. Chem. Chem. Phys.*, 2010
DOI: 10.1039/b924076d

Photoionization of 2-pyridone and 2-hydroxypyridine
J. C. Poully, J. P. Schermann, N. Nieuwjaer, F. Lecomte, G. Grégoire, C. Desfrançois, G. A. Garcia, L. Nahon, D. Nandi, L. Poisson and M. Hochlaf, *Phys. Chem. Chem. Phys.*, 2010
DOI: 10.1039/b923630a

Insulin dimer dissociation and unfolding revealed by amide I two-dimensional infrared spectroscopy
Ziad Ganim, Kevin C. Jones and Andrei Tokmakoff, *Phys. Chem. Chem. Phys.*, 2010
DOI: 10.1039/b923515a

Six conformers of neutral aspartic acid identified in the gas phase
M. Eugenia Sanz, Juan C. López and José L. Alonso, *Phys. Chem. Chem. Phys.*, 2010
DOI: 10.1039/b926520a

Binding a heparin derived disaccharide to defensin inspired peptides: insights to antimicrobial inhibition from gas-phase measurements
Bryan J. McCullough, Jason M. Kalapothakis, Wutharath Chin, Karen Taylor, David J. Clarke, Hayden Eastwood, Dominic Campopiano, Derek MacMillan, Julia Dorin and Perdita E. Barran, *Phys. Chem. Chem. Phys.*, 2010
DOI: 10.1039/b923784d

Guanine–aspartic acid interactions probed with IR–UV resonance spectroscopy
Bridgit O. Crews, Ali Abo-Riziq, Kristýna Pluháčková, Patrina Thompson, Glake Hill, Pavel Hobza and Mattanjah S. de Vries, *Phys. Chem. Chem. Phys.*, 2010
DOI: 10.1039/b925340h

Investigations of the water clusters of the protected amino acid Ac-Phe-OMe by applying IR/UV double resonance spectroscopy: microsolvation of the backbone
Holger Fricke, Kirsten Schwing, Andreas Gerlach, Claus Unterberg and Markus Gerhards, *Phys. Chem. Chem. Phys.*, 2010
DOI: 10.1039/c000424c

Probing the specific interactions and structures of gas-phase vancomycin antibiotics with cell-wall precursor through IRMPD spectroscopy
Jean Christophe Poully, Frédéric Lecomte, Nicolas Nieuwjaer, Bruno Manil, Jean Pierre Schermann, Charles Desfrançois, Florent Calvo and Gilles Grégoire, *Phys. Chem. Chem. Phys.*, 2010
DOI: 10.1039/b923787a

Two-dimensional network stability of nucleobases and amino acids on graphite under ambient conditions: adenine, L-serine and L-tyrosine
Ilko Bald, Sigrid Weigelt, Xiaojing Ma, Pengyang Xie, Ramesh Subramani, Mingdong Dong, Chen Wang, Wael Mamdouh, Jianguo Wang and Flemming Besenbacher, *Phys. Chem. Chem. Phys.*, 2010
DOI: 10.1039/b924098e

Importance of loop dynamics in the neocarzinostatin chromophore binding and release mechanisms
Bing Wang and Kenneth M. Merz Jr., *Phys. Chem. Chem. Phys.*, 2010
DOI: 10.1039/b924951f

Structural diversity of dimers of the Alzheimer Amyloid-(25-35) peptide and polymorphism of the resulting fibrils
Joan-Emma Shea, Andrew I. Jewett, Guanghong Wei, *Phys. Chem. Chem. Phys.*, 2010
DOI: 10.1039/c000755m

Photoelectron spectroscopy of homogeneous nucleic acid base dimer anions

Yeon Jae Ko,[a] Haopeng Wang,[a] Rui Cao,[b] Dunja Radisic,[a] Soren N. Eustis,[a] Sarah T. Stokes,[a] Svetlana Lyapustina,[a] Shan Xi Tian*[b] and Kit H. Bowen*[a]

We report the photoelectron spectra of homogeneous dimer anions of the nucleobases: uracil, thymine, cytosine, adenine, and guanine, i.e., U_2^-, T_2^-, C_2^-, A_2^-, and G_2^- along with DFT calculations on U_2^- and T_2^-. Based on these calculations the photoelectron spectrum of T_2^- was assigned as being due to both a proton transferred and a non-proton transferred isomer, while the photoelectron spectrum of U_2^- was assigned in terms of a single dominant barrier-free proton transferred isomer. Photoelectron spectra were also measured with a different source and on a different type of photoelectron spectrometer for U_2^-, T_2^-, A_2^-, $(1\text{-MeT})_2^-$ and $(1,3\text{-Me}_2U)_2^-$.

I. Introduction

There are several reasons for interest in the electrophilic properties of nucleic acid bases and biomolecular assemblies in which they are moieties, e.g., in DNA. Among these is the relatively recent discovery that very low energy electrons (produced by ionizing radiation as secondary electrons and then thermalized) are capable of breaking both single and double strands of DNA.[1–3] While the detailed mechanism by which this occurs is still under debate, it is generally thought that nucleic acid base moieties within DNA are the electron attachment sites early on in the process.[4–6]

The electrophilic properties of nucleic acid bases have long been studied in condensed phases by EPR spectroscopy.[7] In isolation (gas phase), several experimental and theoretical studies have also investigated the electrophilic properties of nucleobases. Experimentally, these include Rydberg electron transfer, free electron attachment, and anion photoelectron (photodetachment) spectroscopic studies of the naked nucleobases,[8–10] and theoretically, there are even a larger number of studies.[11–15] In addition, hydrated nucleic acid base anions have also been studied by anion photoelectron spectroscopy.[16,17] Moreover, the electrophilic properties of nucleobase pairs have been investigated both experimentally[18–20] and theoretically,[21–23] although most of those studies focused on the heterogeneous $(AT)^-$ and $(GC)^-$ dimer (base pair) anions due to the importance of AT and GC in the genetic code.

The electrophilic properties of homogeneous base pairs, on the other hand, have received relatively less attention, although Rydberg electron transfer studies have probed the valence anion of U_2^-, A_2^-, and T_2^- plus a dipole bound anion state of T_2^-.[24] Here, we report our combined experimental and theoretical studies (photoelectron spectroscopy and density functional theory, respectively) of the homogeneous nucleobase dimer anions, T_2^- and U_2^-, along with the photoelectron spectra of C_2^-, A_2^-, and G_2^-. Our recent development of a source for generating parent (intact) anions of various nucleosides, nucleotides and other biomolecules[25–27] has allowed us to investigate these five homogeneous nucleobase dimer anions. Our computational results are quantitatively consistent with our experimental findings. Both approaches suggest that both T_2^- and U_2^- have multiple anionic isomers.

II. Methods

A Experimental

Anion photoelectron spectroscopy is conducted by crossing a mass-selected, negative ion beam with a fixed-energy photon beam and analyzing the energies of the resultant photodetached electrons. This technique is governed by the well-known energy-conserving relationship, $h\nu = EBE + EKE$, where $h\nu$, EBE, EKE are the photon energy, electron binding energy (transition energy), and the electron kinetic energy, respectively.

Two different types of anion photoelectron spectrometers, each with its own unique anion source, were used to perform these experiments. In one of these, negative ions are generated in an ion source and then travel through a linear, time-of-flight mass spectrometer which serves to provide both mass analysis and mass selection. The mass-selected anions of interest are then photodetached by light from a pulsed laser and their electron kinetic energies are then analyzed with a magnetically-guided electron time-of-flight energy analyzer (a 'magnetic bottle'). Details of our apparatus have been described elsewhere.[28] The third (355 nm, 3.49 eV) harmonic of a Nd:YAG laser was used for the measurements reported in this paper. Photoelectron spectra were calibrated against the well-known photoelectron spectrum of Cu^-. In this apparatus, homogeneous nucleobase dimer anions were generated using our pulsed, infrared desorption-pulsed visible photoemission anion source which we have developed recently.[25] Fragile neutral

[a] Department of Chemistry, Johns Hopkins University, Baltimore, MD 21218, USA. E-mail: kbowen@jhu.edu
[b] Hefei National Laboratory for Physical Sciences at Microscale and Department of Chemical Physics, University of Science and Technology of China, Hefei, Anhui 230026, China. E-mail: sxtian@ustc.edu.cn

biomolecules were brought into the gas phase by infrared desorption, while at almost the same time low energy electrons were generated by photoemission and a jet of helium (4N4 grade) was fired to provide collisional cooling. Desorption of involatile biomolecules was accomplished by directing a low power pulse of first harmonic (1064 nm, 1.16 eV) Nd:YAG laser light onto a translating graphite bar, thinly coated with the nucleobase of interest. Low energy electrons were emitted by coordinating a strong pulse of second harmonic (532 nm, 2.33 eV) Nd:YAG light onto a rotating yttrium oxide (work function of *ca.* 2 eV) disk. The helium jet was generated in a standard pulsed valve.

In the other type of spectrometer, negative ions were mass-analyzed and mass-selected with a 90° magnetic sector before being crossed with the beam of an argon ion laser, operating intracavity at 2.54 eV per photon.[29] The electron kinetic energies of resulting photoelectrons were then analyzed by a hemispherical electron energy analyzer. In contrast to the pulsed operation of the spectrometer described above, all components of this type pd photoelectron spectrometer operate continuously. Photoelectron spectra were calibrated against the well-known spectrum of O^-. To prepare the nucleobase dimer anions of interest, nucleic acid bases were evaporated thermally (180–200 °C) in an argon-filled stagnation chamber before being expanded into high vacuum through a small nozzle. Low energy electrons, emitted from a negatively biased thoriated-iridium filament, were then injected into the resulting jet, forming a weak magnetically-supported plasma. Negative ions produced in this way, *i.e.*, in a nozzle-ion source, were then extracted into the ion optics of the spectrometer's beam-line for transport into the magnetic sector described above. This apparatus differs from the other one used in these experiments in that it and its source operate continuously, while the earlier discussed spectrometer and its source operate in a pulsed mode.

B   Computational

There are six possible sets of double, hydrogen bond interactions between the nucleobases in a homogeneous nucleobase dimer. The geometrical parameters of all six sets were fully optimized at the B3LYP[30,31]/6-31++G(d,p) level of theory for both neutral and anionic, homogeneous uracil and thymine dimers. Some of these are the products of proton transfer (PT) events between two paired canonical bases. The geometrical parameters of the transition states for the PT processes were optimized with the STQN method[32] and further confirmed with IRC calculations. The vertical detachment energy (VDE) of the anion was calculated as $VDE = E_{tot}^n(anion) - E_{tot}^a$ (anion), where the energy of the neutral dimer, E_{tot}^n, was calculated at the anionic geometry. The adiabatic electron affinity (EA_a) of the neutral was calculated as $EA_a = E_{tot}^n$ (neutral) $- E_{tot}^a$(anion), where the total energies of two monomers were calculated at their respective equilibrium structures and corrected for the zero-point vibrational energies (ZPVEs). In order to explore the proton transfer processes for both the neutral and anionic dimers, the relaxed potential energy profiles were obtained by controlling the variation of the specific N–H bond length along with optimizing the

geometrical parameters of the other moieties. All above calculations were performed with Gaussian 03 program.[33] The molecular structures and the electron density maps were depicted with the MOLDEN program.[34]

The symbols used throughout the text for denoting hydrogen-bonded nucleobase dimers are similar to those originally presented by Gutowski *et al.*[18] The prefixes "a" and "n" stand for anionic and neutral dimers, respectively, while the superscripts and subscripts following the letter symbol of a given nucleobase indicate how the hydrogen bonds were formed. Using $aT_{N1}^{O7}T_{O8-H}^{N3}$ as an example shown in Fig. 1, the anionic thymine dimer has a hydrogen bond between the O7 site of the left-most thymine and the hydrogen atom on the N3 site of the other thymine, and another hydrogen bond between the N1 site of the former and the O8 site of the latter, where the O8–H symbol denotes that a proton transfer has taken place from the N1 site to the O8 site.

III.   Results

Photoelectron spectra of the five homogeneous nucleobase dimer anions generated with an infrared desorption/photoemission source and measured on our pulsed apparatus are presented in Fig. 2. The photoelectron spectra of the three pyrimidine dimer anions [see Fig. 2(a) through (c)] each exhibit a dominant broad peak well within the energy window of the spectra, before their intensities gradually increase toward the high electron binding energy (EBE) ends of their spectra. Generally, their intensity thresholds occur at EBE ≈ 0.7 eV. In the case of T_2^-, a weaker intensity, broad peak is also discernible at EBE ≈ 2.3 eV, and in the case of U_2^-, there is a shoulder on the low EBE side of the main peak. The photoelectron spectra of the two purine dimer anions [see Fig. 2(d) and (e)] have similar spectral patterns, with each exhibiting two peaks. In both spectra these peaks are separated by ~ 0.9 eV, and in both spectra the two peaks exhibit about the same intensity ratios. They differ, however, in that the spectrum of A_2^- is shifted to higher EBE by ~ 0.5 eV relative to the spectrum of G_2^-.

Photoelectron spectral results are also shown in Fig. 3, where variations in T_2^- spectra are examined under varied pulsed gas valve durations (under varied source conditions). Fig. 4 compares the photoelectron spectra of T_2^-, U_2^-, and A_2^-, generated in a nozzle-ion source and measured on our continuous photoelectron spectrometer, with their corresponding photoelectron spectra generated in an infrared desorption/photoemission source and measured on our pulsed spectrometer. Lastly, Fig. 5 compares the photoelectron spectrum of U_2^- with its methylated derivatives having different degrees and/or sites of methylation. The first two spectra in Fig. 5(a) and (b) are the same spectra shown in Fig. 2, while the latter two in Fig. 5(c) and (d) were generated in a nozzle-ion source and measured on our continuous photoelectron spectrometer.

Computational results are presented in Table 1. These results show that the three low-lying anionic thymine dimers, *i.e.*, $aT_{N1}^{O7}T_{O8-H}^{N3}$ (C_1 symmetry), $aT_{N1}^{O7}T_{O8}^{N3}$ (C_1 symmetry), and $aT_{N1}^{O7}T_{O7}^{N1}$ (C_{2h} symmetry), and the two low-lying anionic uracil dimers, *i.e.*, $aU_{N1}^{O7}U_{O8-H}^{N3}$ (C_1 symmetry) and $aU_{N1}^{O7}U_{O7}^{N1}$
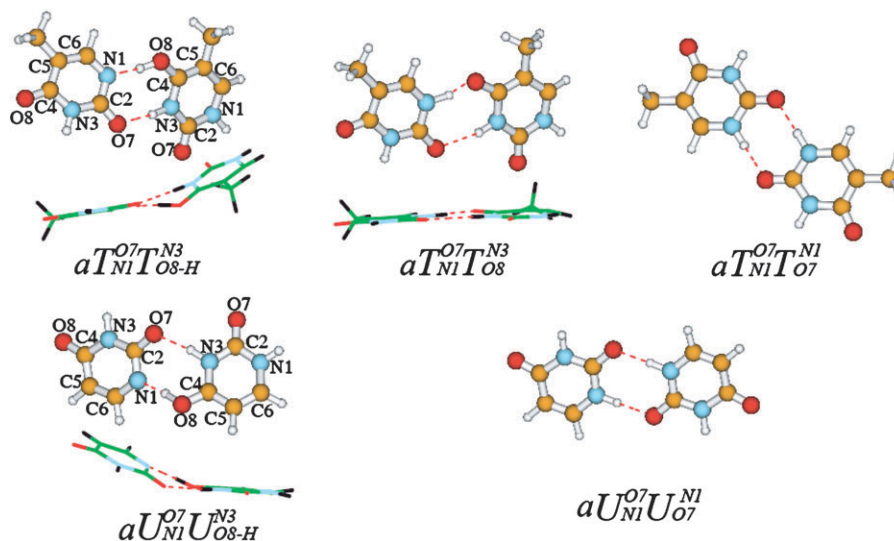
Fig. 1 Dominant anionic dimers of thymine (upper) and uracil (lower).
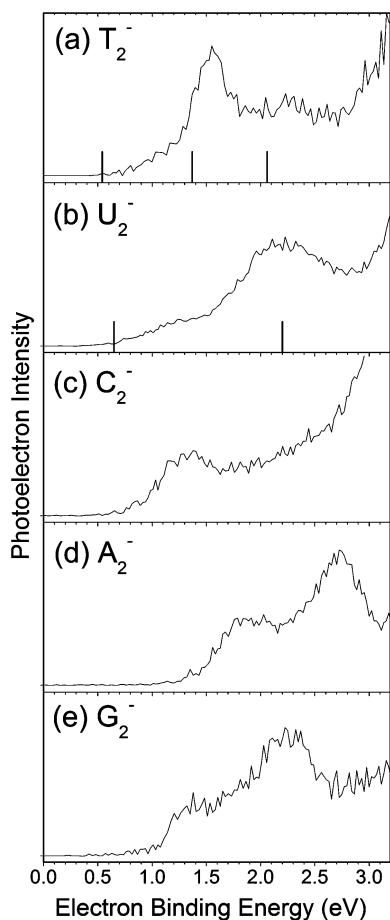

Fig. 2 Photoelectron spectra of homogeneous nucleobase dimer anions (a)–(e) recorded with 355 nm (3.49 eV) photons. VDE calculations of T_2^- and U_2^- are shown as stick spectra in (a) and (b), respectively.

Fig. 3 Photoelectron spectra of T_2^- recorded with 355 nm photons at three different pulsed gas valve durations. Pressure of the carrier gas (He) was constant at 200 psi.

(C_{2h} symmetry), are the major calculated configurations of these anionic dimers. Their geometric structures are presented in Fig. 1. In order to model the experimental environment due
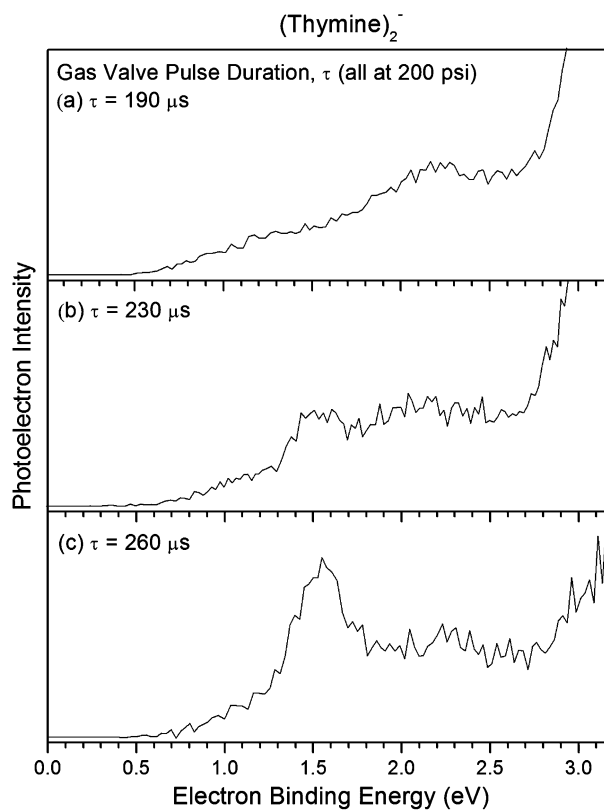
to cooling by the helium gas jet, we conducted an additional calculation to estimate the temperature dependence of the relative abundance of the gas phase isomers of T_2^- and U_2^-. The percentage contributions (at temperatures, 250, 453, and 473 K) of the different isomers were estimated using a Boltzmann function, $\exp(\Delta E_{tot}^{-ZPVE}/RT)$, where ΔE_{tot} is the total energy difference between the most stable dimeric form and the others (the ZPVE corrections are included), and R is

This journal is © the Owner Societies 2010

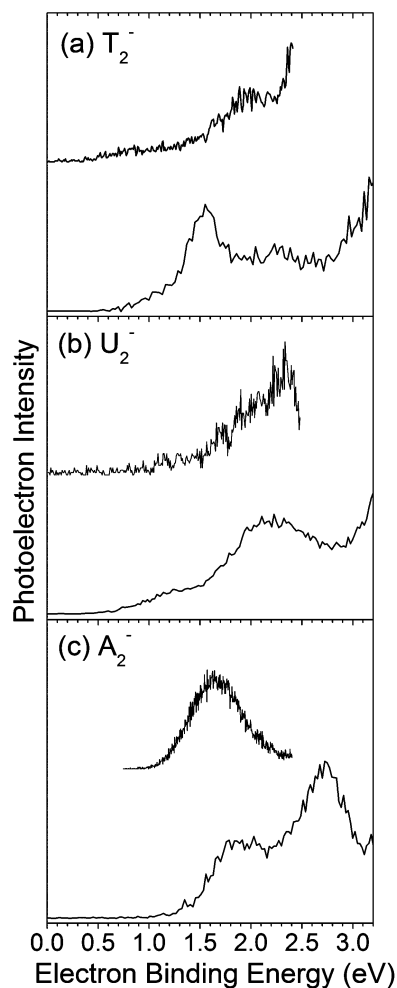*Phys. Chem. Chem. Phys.*, 2010, **12**, 3535–3541 | 3537

Fig. 4 Comparison of the photoelectron spectra of T_2^-, U_2^-, and A_2^- generated both by our infrared desorption/photoemission source and by our thermal nozzle-ion source.

Fig. 5 Comparison of the anion photoelectron spectra of U_2^-, T_2^-, $(1\text{-MeT})_2^-$ and $(1,3\text{-Me}_2\text{U})_2^-$.

the gas constant. These relative contributions are shown in Table 1. According to our calculations, the newly formed, "hot" dimer anion (at 453 and 473 K) should have three stable T_2^- isomers, *i.e.*, $aT_{N1}^{O7}T_{O8-H}^{N3}$, $aT_{N1}^{O7}T_{O8}^{N3}$, and $aT_{N1}^{O7}T_{O7}^{N1}$, and two stable U_2^- isomers, $aU_{N1}^{O7}U_{O8-H}^{N3}$ and $aU_{N1}^{O7}U_{O7}^{N1}$. After these dimer anions are cooled by series of collisions with the carrier gas at 250 K, $aT_{N1}^{O7}T_{O8-H}^{N3}$, $aT_{N1}^{O7}T_{O8}^{N3}$, and $aU_{N1}^{O7}U_{O8-H}^{N3}$ become dominant. The calculated VDE values of these three dimer anions match fairly well the peak centers of the main features in the spectra of T_2^- and U_2^- (see Fig. 2), where stick spectra denote the calculated transitions. Calculated VDE values for the other two dimer anions mentioned above may correspond to the intensity thresholds at EBE ≈ 0.7 eV, and they are also marked by stick spectra in Fig. 2. Since the spectra of C_2^-, A_2^- and G_2^- were also measured in the same source environments, it is likely that they were produced at similar temperatures.

IV. Discussion

In the photoelectron spectrum of T_2^- [see Fig. 2(a)], the peak centered at EBE = 1.55 eV is assigned as arising from the
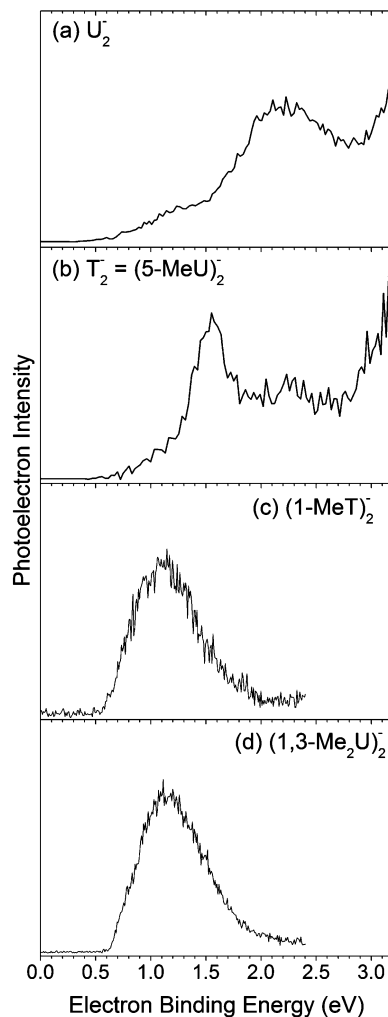
photodetachment of $aT_{N1}^{O7}T_{O8}^{N3}$ (predicted to occur at 1.37 eV), while the feature centered around EBE ≈ 2.3 eV is assigned as arising from the photodetachment of $aT_{N1}^{O7}T_{O8-H}^{N3}$ (predicted at 2.06 eV). The threshold feature starting near EBE ≈ 0.7 eV may be due to the photodetachment of $aT_{N1}^{O7}T_{O7}^{N1}$ (predicted at 0.54 eV). In the photoelectron spectrum of U_2^- [see Fig. 2(b)], the peak centered at EBE = 2.2 eV is assigned as arising from the photodetachment of $aU_{N1}^{O7}U_{O8-H}^{N3}$ (predicted to occur at 2.20 eV). The threshold feature starting near EBE ≈ 0.7 eV may be due to the photodetachment of $aU_{N1}^{O7}U_{O7}^{N1}$ (predicted at 0.65 eV). Since computational results are not available for C_2^-, A_2^-, and G_2^-, spectral assignments of those photoelectron spectra have not been made.

The underlying natures of $aU_{N1}^{O7}U_{O8-H}^{N3}$, $aT_{N1}^{O7}T_{O8-H}^{N3}$, and $aT_{N1}^{O7}T_{O8}^{N3}$ are elucidated by the computational results presented in Fig. 6 and 7. The potential curves in Fig. 6(a) show that $aU_{N1}^{O7}U_{O8-H}^{N3}$ was formed by a barrier-free proton transfer. The curves in Fig. 6(b) show that the proton transfer which formed $aT_{N1}^{O7}T_{O8-H}^{N3}$ involved a slight barrier, *i.e.*, it was not barrier-free. The formation of $aT_{N1}^{O7}T_{O8}^{N3}$, on the other hand, did not involve proton transfer. Thus, the photoelectron spectrum of T_2^- shows evidence for the formation of both a

Table 1 Relative stabilities (δE), vertical detachment energies (VDE), and relative percentages of the gas phase anionic dimers, and electron affinities (EA) of the gas phase neutral dimers

Anionic dimers	δE/kcal mol^{-1}	VDE/eV	Percentage at temperature T			Neutral dimers	EA/eV
			250.15 K	453.15 K	473.15 K		
$aT_{N1}^{O7}T_{O8-H}^{N3}$	0.00	2.06	89.8%	72.7%	71.4%	$nT_{N1}^{O7}T_{O8}^{N3}$	0.76[a]
$aT_{N1}^{O7}T_{O8}^{N3}$	1.15	1.37	8.9%	20.3%	21.0%	—	0.71[b]
$aT_{N1}^{O7}T_{O7}^{N1}$	2.11	0.54	1.3%	6.9%	7.6%	$nT_{N1}^{O7}T_{O7}^{N1}$	0.52
$aT_{N1}T_{O7}$	7.91	1.26	—	—	—	$nT_{N1}^{O7}T_{O7}^{N3}$	0.44
$aT_{N3}^{O8}T_{O8}^{N3}$	10.00	0.42	—	—	—	$nT_{N3}^{O8}T_{O8}^{N3}$	0.44
$aT_{N3}^{O7}T_{O8}^{N3}$	11.21	0.40	—	—	—	$nT_{N3}^{O7}T_{O8}^{N3}$	0.40
$aT_{N3}^{O7}T_{O7}^{N3}$	13.00	0.32	—	—	—	$nT_{N3}^{O7}T_{O7}^{N3}$	0.34
$aU_{N1}^{O7}U_{O8-H}^{N3}$	0.00	2.20	99.6%	95.5%	94.9%	$nU_{N1}^{O7}U_{O8}^{N3}$	0.87
$aU_{N1}^{O7}U_{O7}^{N1}$	2.75	0.65	0.4%	4.5%	5.1%	$nU_{N1}^{O7}U_{O7}^{N1}$	0.63
$aU_{N1}^{O7}U_{O7}^{N3}$	8.16	0.99	—	—	—	$nU_{N1}^{O7}U_{O7}^{N3}$	0.57
$aU_{N3}^{O8}U_{O8}^{N3}$	10.95	0.50	—	—	—	$nU_{N3}^{O8}U_{O8}^{N3}$	0.52
$aU_{N3}^{O7}U_{O8}^{N3}$	12.21	0.20	—	—	—	$nU_{N3}^{O7}U_{O8}^{N3}$	0.50
$aU_{N3}^{O7}U_{O7}^{N3}$	13.89	0.17	—	—	—	$nU_{N3}^{O7}U_{O7}^{N3}$	0.44

^{a} With respect to $aT_{N1}^{O7}T_{O8-H}^{N3}$. ^{b} With respect to $aT_{N1}^{O7}T_{O8}^{N3}$.

proton transferred and a non-proton transferred thymine dimer anion. Fig. 7 presents electron density maps for the highest singly-occupied molecular orbitals (SOMOs) of these three anionic dimers. The unpaired electron resides on one of the two molecules in a given dimer, and these SOMO's have π orbital characteristics.

We now turn to three different comparisons of our spectroscopic data. The particular tautomeric isomers that form depend both on the type of anion source used and on the different source conditions available within a given source.
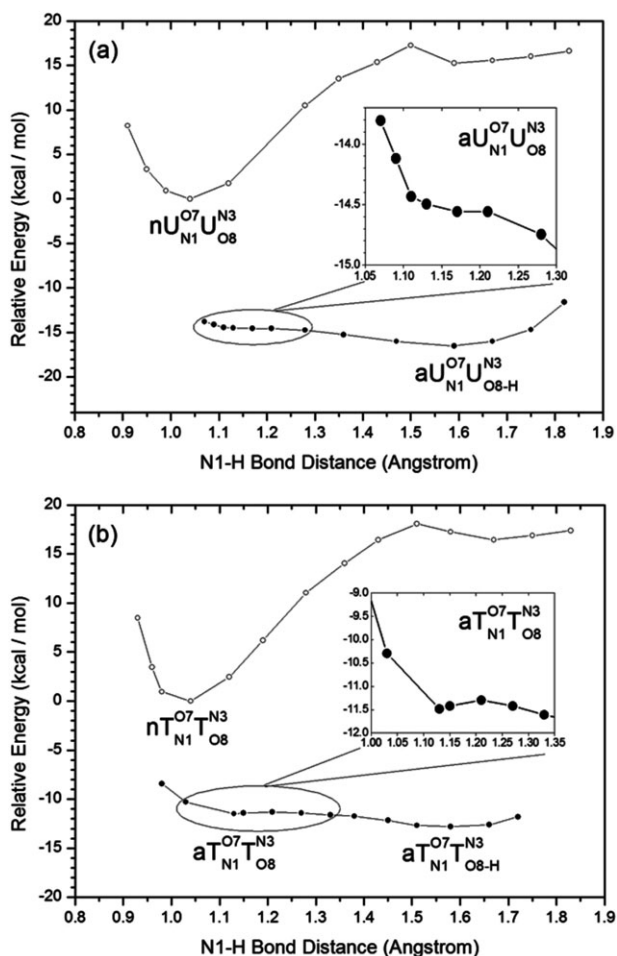

Fig. 6 Relaxed energy profiles generated by scanning the N1–H bond length for the neutral (outlined dots) and anionic (solid dots) dimers of uracil (a) and thymine (b).
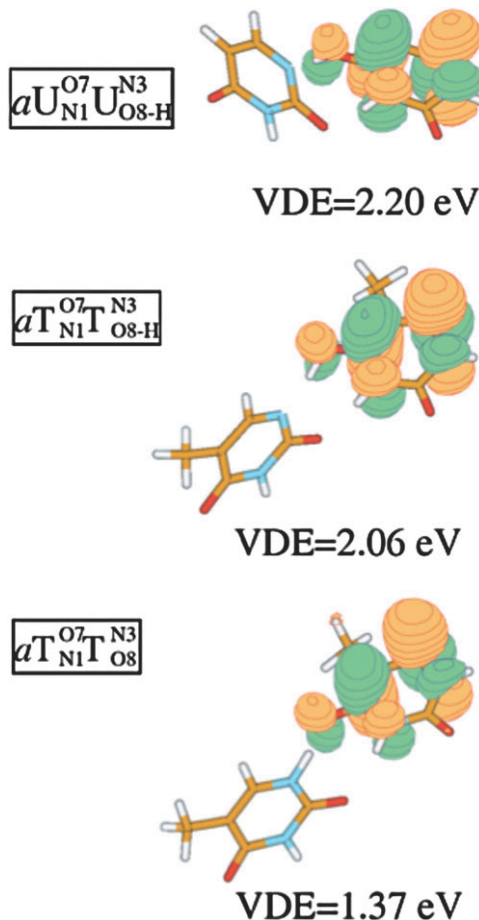

Fig. 7 Electron density maps for the highest singly-occupied molecular orbitals of the dominant anionic dimers.

This journal is © the Owner Societies 2010

Phys. Chem. Chem. Phys., 2010, **12**, 3535–3541 | 3539

While the relative intensities of peaks varied to some degree for all five nucleobase dimer anions studied, the behavior of T_2^- was the most dramatic. Fig. 3 shows how the photoelectron spectrum of T_2^- changed with gas valve pulse durations. Longer gas pulse durations presumably resulted in greater cooling. One sees that the proton transferred $aT_{N1}^{O7}T_{O8-H}^{N3}$ dimer anion forms even at short pulse durations (relatively warm conditions), but that the non-proton transferred $aT_{N1}^{O7}T_{O8}^{N3}$ dimer anion grows in strongly with longer pulse durations and more cooling. This is reasonable since our calculations predict that $aT_{N1}^{O7}T_{O8-H}^{N3}$ is the most stable of the T_2^- isomers.

In addition to the five dimer anions which were generated in our infrared desorption/photoemission source and studied on our pulsed photoelectron spectrometer, the dimer anions, T_2^-, U_2^-, and A_2^-, were also generated in a nozzle-ion source and studied on our continuous photoelectron spectrometer. In Fig. 4, we compare the photoelectron spectra of these three dimer anions formed and measured on different types of photoelectron apparatus. Due to the use of an argon ion laser on the continuous machine, the photoelectron spectra measured there span only an electron binding energy range up to ~ 2.4 eV. Nevertheless, it is still possible to make several comparisons. The T_2^- spectrum taken on the continuous spectrometer resembles the T_2^- spectrum taken on the pulsed spectrometer under short gas duration (warm) conditions, suggesting that the nozzle expansion in the former case did not cool well. The spectra of U_2^- taken on both apparatus are relatively consistent. Both spectra of A_2^- show bands in the same energy region but with an offset of ~ 0.2 eV. While peak-pulling of the band in question in the lower (pulsed apparatus) spectrum is doubtless a factor in the apparent band shift, the fact that the upper (continuous apparatus) spectrum shows no hint (on its high EBE side) of the higher EBE band seen in the pulsed apparatus spectrum suggests that the two different anion sources may not have generated entirely the same A_2^- isomers.

In addition to T_2^-, U_2^-, and A_2^- which were generated and studied on our continuous apparatus, we also generated and studied (1-methylthymine)$_2^-$ and (1,3 dimethyluracil)$_2^-$ in the same way on the same apparatus. Their photoelectron spectra are presented in Fig. 5 along with those of U_2^- and T_2^- measured on the pulsed apparatus. From the top to bottom in Fig. 5, the spectra are arranged in order of increasing methylation, i.e., molecules of U have no methyl groups, those of T have one, while those of 1-MeT and 1,3-Me$_2$U have two methyl groups each. We make the following observations/ speculations. The bands at EBE = 2.2 eV and 2.3 eV in U_2^- and T_2^-, respectively, have essentially the same proton transfer configurations, i.e., $aU_{N1}^{O7}U_{O8-H}^{N3}$ and $aT_{N1}^{O7}T_{O8-H}^{N3}$. Moreover, they are insensitive to methylation. The lower EBE band (at EBE = 1.55 eV) in the T_2^- spectrum comes from the photo-detachment of the $aT_{N1}^{O7}T_{O8}^{N3}$ configuration, which is similar to the above configurations, except that it does not give rise to proton transfer. The occurrence of this particular isomer of T_2^- is rooted in the presence of a methyl group in thymine. We saw a similar effect when we methylated adenine and thymine at their sugar positions, tieing-up these sites and inhibiting proton transfer in [(MeA)(MeT)]$^-$ even though it had been

evident in (AT)$^-$.[18] We suspect that more of the same is occurring in the observed spectral bands of (1-MeT)$_2^-$ and (1,3-Me$_2$U)$_2^-$, and that these are also due to non-proton transferred isomers.

References

1 B. Boudaiffa, P. Cloutier, D. Hunting, M. A. Huels and L. Sanche, Science, 2000, **287**, 1658.
2 F. Martin, P. D. Burrow, Z. Cai, P. Cloutier, D. Hunting and L. Sanche, Phys. Rev. Lett., 2004, **93**, 068101.
3 L. Sanche, Mass Spectrom. Rev., 2002, **21**, 349.
4 J. Rak, K. Mazurkiewicz, M. Kobylecka, P. Storoniak, M. Haranczyk, I. Dabkowska, R. A. Bachorz, M. Gutowski, D. Radisic, S. T. Stokes, S. N. Eustis, D. Wang, X. Li, Y. J. Ko and K. H. Bowen, in Radiation Induced Molecular Phenomena in Nucleic Acids: A Comprehensive Theoretical and Experimental Analysis, ed. M. K. Shukla and J. Leszczynski, Springer-Verlag, Amsterdam, 2008, vol. 5.
5 J. Simons, Acc. Chem. Res., 2006, **39**, 772.
6 X. Li, M. D. Sevilla and L. Sanche, J. Am. Chem. Soc., 2003, **125**, 13668.
7 M. D. Sevilla and D. Becker, Royal Society of Chemistry Special Review on Electron Spin Resonance, Royal Society of Chemistry, Cambridge, UK, 1994, vol. 14, ch. 5.
8 C. Desfrancois, H. Abdoul-Carime and J. P. Schermann, J. Chem. Phys., 1996, **104**, 7792.
9 S. Ptasinska, S. Denifl, B. Mroz, M. Probst, V. Grill, E. Illenberger, P. Sceoer and T. D. Maerk, J. Chem. Phys., 2005, **123**, 124302.
10 J. H. Hendricks, S. A. Lyapustina, H. L. de Clercq, J. T. Snodgrass and K. H. Bowen, J. Chem. Phys., 1996, **104**, 7788.
11 S. S. Wesolowski, M. L. Leninger, P. N. Penchev and H. F. Schaefer, J. Am. Chem. Soc., 2001, **123**, 4023.
12 X. Li, Z. Cai and M. D. Sevilla, J. Phys. Chem. A, 2002, **106**, 1596.
13 R. A. Bachorz, J. Rak and M. Gutowski, Phys. Chem. Chem. Phys., 2005, **7**, 2116.
14 O. Dolgounitcheva, V. G. Zakrzewski and J. V. Ortiz, Chem. Phys. Lett., 1999, **307**, 220.
15 C. Winsted and V. McKoy, J. Chem. Phys., 2006, **125**, 174304.
16 J. Schiedt, R. Weinkauf, D. M. Neumark and E. W. Schlag, Chem. Phys., 1998, **239**, 511.
17 S. N. Eustis, D. Wang, S. Lyapustina and K. H. Bowen, J. Chem. Phys., 2007, **127**, 224309.
18 D. Radisic, K. H. Bowen, I. Dabkowska, P. Storoniak, J. Rak and M. Gutowski, J. Am. Chem. Soc., 2005, **127**, 6443.
19 A. Szyperska, J. Rak, J. Leszczynski, X. Li, Y. J. Ko, H. Wang and K. H. Bowen, J. Am. Chem. Soc., 2009, **131**, 2663.
20 A. Szyperska, J. Rak, J. Leszczynski, X. Li, Y. J. Ko, H. Wang and K. H. Bowen, ChemPhysChem, 2010, DOI: 10.1002/ cphc.200900810.
21 N. A. Richardson, S. S. Wesolowski and H. F. Schaefer, III, J. Am. Chem. Soc., 2002, **124**, 10163.
22 X. Li and M. D. Sevilla, Adv. Quantum Chem., 2007, **52**, 59.
23 C. Desfrancois, S. Carles and J. P. Schermann, Chem. Rev., 2000, **100**, 3943.
24 C. Desfrancois, H. Abdoul-Carime, C. P. Schulz and J. P. Schermann, Science, 1995, **269**, 1707.
25 S. T. Stokes, X. Li, A. Grubisic, Y. J. Ko and K. H. Bowen, J. Chem. Phys., 2007, **127**, 084321.
26 S. T. Stokes, A. Grubisic, X. Li, Y. J. Ko and K. H. Bowen, J. Chem. Phys., 2008, **128**, 044314.

3540 | Phys. Chem. Chem. Phys., 2010, **12**, 3535–3541

This journal is © the Owner Societies 2010

27 M. Seydou, J. C. Gillet, X. Li, H. Wang, G. H. Posner, G. Gregoire, J. P. Schermann, K. H. Bowen and C. Desfrancois, *Chem. Phys. Lett.*, 2007, **449**, 286.

28 M. Gerhards, O. C. Thomas, J. M. Nilles, W.-J. Zheng and K. H. Bowen, *J. Chem. Phys.*, 2002, **116**, 10247.

29 J. V. Coe, J. T. Snodgrass, C. B. Friedhoff, K. M. McHugh and K. H. Bowen, *Chem. Phys.*, 1986, **84**, 618.

30 A. D. Becke, *J. Chem. Phys.*, 1993, **98**, 5648.

31 C. Lee, W. Yang and R. G. Parr, *Phys. Rev. B: Condens. Matter*, 1988, **37**, 785.

32 Æ. Frisch and M. J. Frisch, *GAUSSIAN 98 User's Reference*, Gaussian, Inc., Pittsburg, 1998.

33 M. J. Frisch, G. W. Trucks, H. B. Schlegel, G. E. Scuseria, M. A. Robb, J. R. Cheeseman, J. A. Montgomery, Jr., T. Vreven, K. N. Kudin, J. C. Burant, J. M. Millam, S. S. Iyengar, J. Tomasi, V. Barone, B. Mennucci, M. Cossi, G. Scalmani, N. Rega, G. A. Petersson, H. Nakatsuji, M. Hada, M. Ehara, K. Toyota, R. Fukuda, J. Hasegawa, M. Ishida, T. Nakajima, Y. Honda, O. Kitao, H. Nakai, M. Klene, X. Li, J. E. Knox, H. P. Hratchian, J. B. Cross, C. Adamo, J. Jaramillo, R. Gomperts, R. E. Stratmann, O. Yazyev, A. J. Austin, R. Cammi, C. Pomelli, J. W. Ochterski, P. Y. Ayala, K. Morokuma, G. A. Voth, P. Salvador, J. J. Dannenberg, V. G. Zakrzewski, S. Dapprich, A. D. Daniels, M. C. Strain, O. Farkas, D. K. Malick, A. D. Rabuck, K. Raghavachari, J. B. Foresman, J. V. Ortiz, Q. Cui, A. G. Baboul, S. Clifford, J. Cioslowski, B. B. Stefanov, G. Liu, A. Liashenko, P. Piskorz, I. Komaromi, R. L. Martin, D. J. Fox, T. Keith, M. A. Al-Laham, C. Y. Peng, A. Nanayakkara, M. Challacombe, P. M. W. Gill, B. Johnson, W. Chen, M. W. Wong, C. Gonzalez and J. A. Pople, *GAUSSIAN 03 (Revision C.02)*, Gaussian, Inc., Wallingford, 2004.

34 G. Schaftenaar, *MOLDEN 3.4*, CAOS/CAMM Center, The Netherlands, 1998.